

Electronic Supplementary Information

Fe-TCPP@CS Nanoparticles as Photodynamic and Photothermal Agent for Efficient Antimicrobial Therapy

Yufeng Zhang,^{a,b} Jing Ma,^{a,b} Dianwei Wang,^b Caina Xu,^b Shu Sheng,^b Jianfeng Cheng,^a Changjiang Bao,^a

Yanhui Li^{*a} and Huayu Tian^{*b}

^a. School of Materials Science and Engineering, Changchun University of Science and Technology, Changchun 130022, China

^b. Key Laboratory of Polymer Ecomaterials, Changchun Institute of Applied Chemistry, Chinese Academy of Sciences, Changchun 130022, China

Experimental procedures

Chemicals and reagents: Methyl terephthalaldehyde, pyrrole, sodium acetate trihydrate, Iron (III) chloride hexahydrate and Vitamin C (VC) were purchased from Aladdin (Shanghai, China). Chitosan (MW=30000, deacetylation degree > 95 %) was obtained from Macklin (Shanghai, China). 9,10-anthracenediyl-bis(methylene)dimalonic acid (ABDA) was purchased from Sigma-Aldrich Inc. (Shanghai, China). Singlet oxygen sensor green (SOSG) was obtained from Dalian Meilun Biotechnology Co., LTD. (Dalian, China). SYTO9 and propidium iodide were purchased Shanghai Beinuo Biotechnology Co., LTD. (Shanghai, China).

Instruments: Zeta potential and size of nanoparticles were measured by zeta potential/BI-90Plus particle size analyzer (Brookhaven, USA). Scanning electron microscopy (SEM) image was gained by field emission scanning electron microscope (Zeiss Merlin FE-SEM). Fourier-transform infrared spectroscopy (FTIR) spectra were obtained from Nicolet 520 FTIR spectrometer. The UV-vis-NIR spectra were obtained by spectrophotometer (U-4100, Hitachi, Japan). The fluorescence intensity was measured using a fluorometer (Photon Technology International Inc., Canada). The content of Fe element was detected by inductively coupled plasma mass spectroscopy (ICP-MS) (PerkinElmer, USA). ¹H NMR spectra were recorded on an AV-300 NMR spectrometer (Bruker, Karlsruhe, Germany) in dimethyl sulphoxide (DMSO). The optical density of bacteria was measured by an enzyme marker (TECAN, Switzerland).

Synthesis of Fe-TCPP@CS NPs: The porphyrinic ligand was prepared according to the reported procedure and ¹H-NMR spectrum of TCPP as shown in Figure S2a was consistent with the literature reports.¹ The [Fe₃O(OOCCH₃)₆OH]·2H₂O SBU was synthesized based on a reported procedure,² and the FT-IR spectrum of [Fe₃O(OOCCH₃)₆OH]·2H₂O as shown in Figure S2b. The structures of TCPP and Fe₃O cluster were shown in Figure S1. For preparing Fe-TCPP@CS, 55 mg of Fe₃O and 33 mg of TCPP were dissolved in 50 mL of DMF assisted by sonication; afterwards, 5 mL of formic acid was added to the above solution. The uniform reaction mixture was transferred into a single-necked flask, stirred and heated to 80 °C for 24 h. The purple precipitate (Fe-TCPP) was collected by centrifugation (10,000 rpm) and washed with DMF and ethanol. To prepare CS solution, 1 g of CS (MW=30000, deacetylation degree > 95 %) was dissolved in 100 mL of acetic acid solution (1 wt %) with continuous mechanical stirring for 6 h to obtain a homogeneous viscous mixture. Then, to a 50 mL glass vial was added 5 mL of Fe-TCPP suspension (8 mg/mL) and 15 mL of CS solution (10 mg/mL). The reaction mixture was stirred for 12 hours at room temperature. The Fe-TCPP@CS was washed and collected by centrifugation (10,000 rpm).

Photodynamic Effect of Fe-TCPP@CS NPs: Fe-TCPP@CS NPs suspension was prepared with a dose of 10 µg/mL (final concentration) and ABDA was added (final concentration= 40 µg/mL) before the UV-vis absorption spectrum measurements. The mixed solution was exposed to white light (30 mW/cm²) and laser (635nm, 1 W/cm²) for 0, 2, 4, 6, 8 and 10 min, and the UV-vis absorption spectrum at different time points was measured. To further determine ROS generation, the fluorescence intensity of a ¹O₂ probe, SOSG was added (final concentration=12.5 µM) before fluorescence measurements. The mixed solution was exposed to white light (30 mW/cm²) and laser (635 nm, 1 W/cm²) for 0 and 5 min, and the fluorescence was measured by a fluorimeter.

Photothermal Effect of Fe-TCPP@CS NPs: The photothermal effect of Fe-TCPP@CS NPs was studied by monitoring the temperature changes of Fe-TCPP@CS NPs aqueous dispersions of different concentrations exposed to a 635 nm laser (1 W/cm²) and using an infrared thermal camera recorded the real-time temperatures. The thermal stability of the Fe-TCPP@CS NPs suspension was evaluated by irradiating for 10 min each time and then naturally cooling to room temperature. The cycle was repeated three times. The photothermal conversion efficiency of Fe-TCPP@CS NPs was calculated according to the following steps.

Photothermal conversion efficiency (η) can be calculated as eq (1).³

$$\eta = \frac{hS(T_{max} - T_0) - Q_0}{I(1 - 10^{-A_\lambda})} \times 100\% \quad (1)$$

Where T_{max} of the equilibrium temperature is 43.7 °C. T_0 of the ambient temperature is 27.5 °C. Q_0 is the baseline energy input of the sample cell. I of the laser power is 1.0 W/cm². A_{635} of the absorption intensity of NPs at 635 nm is 0.3. h is the heat transfer coefficient. S is the surface area of the sample well. hS can be determined by the eq (2).

$$hS = \frac{\sum_i C_{p,i} m_i}{\tau_s} \quad (2)$$

Where the mass of the sample solution (m) is 0.2 g, the heat capacity value (C) of the sample is about 4.2 J g⁻¹ K⁻¹. τ_s is the slope of the line in Figure S8a, which was determined as 151.8. Substituting hS into eq (1), the η of nanoprobe could be calculated to be 18 %.

Antibacterial Experiment: The antibacterial efficiency of Fe-TCPP@CS NPs was evaluated using a spread plate method. *S. aureus*, *E. coli* and MRSA were selected and cultured in fresh medium for 10 h on a 37 °C constant temperature shaker. The bacteria in the log phase were diluted with fresh medium, and the bacteria (100 μL, 10⁶ CFU/mL) were added to a 96-well plate. Then, PBS, VC, Fe-TCPP NPs and Fe-TCPP@CS NPs were added to a 96-well plate separately and cultured for 0.5 h. After coincubation, the light groups were exposed to white light (30 mW/cm²) for *S. aureus* and MRSA, and 635 nm laser (1.0 W/cm²) for *E. coli*. The bacteria solution was diluted after irradiation and 100 μL of diluted bacterial solution was spread on a solid medium. The plates were cultured at 37 °C for 12 h and the number of colony forming units (CFUs).

Then the above bacterial suspension after various treatments was collected via centrifugation and washed with PBS. Ten microliter of PI and SYTO9 were simultaneously incubated with 20 μL of the obtained bacterial suspension in the dark for 20 min at room temperature. PI can only stain damaged bacterial membrane structures with red fluorescence, whereas SYTO9 can enter all bacteria and let it stain green fluorescence.

In Vitro Cytotoxicity Assay: The *in vitro* cytotoxicity of Fe-TCPP@CS was evaluated by a standard 3-(4,5-dimethylthiazol-2-yl)-2,5-diphenyltetrazolium bromide (MTT) assay on mouse embryonic fibroblast cells (3T3 cells). The cells were seeded in 96-well plates and incubated for 12 h. Then, Fe-TCPP@CS NPs with different concentrations was added to incubate with cells. After 6 h, MTT solution was used to measure the viability of cells.

Hemolytic Assay: Hemolysis assay was conducted on red blood cells (RBCs) of rabbit (4 %). First, the RBCs (5 ml) were rinsed with PBS (0.02 M, pH = 7.4) three times and collected by centrifugation (1,500 rpm, 5 min). Next, the RBCs were added into 5 mL of PBS to prepare the stock dispersion. Then, 400 μL of stock dispersion was added to 400 μL of different concentrations of Fe-TCPP@CS NPs and the solutions were incubated at 37 °C for 4 h after irradiation. The percentage of hemolysis was measured by UV-vis analysis of the supernatant at 576 nm absorbance after centrifugation at 2,000 rpm for 10 min. The deionized water treatment group was used as a positive control group, and the PBS treatment group acted as a negative control group. The hemolysis percentage was calculated using the following formula:

$$\text{hemolysis ratio (\%)} = (A_S - A_N) / (A_P - A_N) \times 100\%$$

where, A_S , A_N , and A_P represent the absorbance of Fe-TCPP@CS treatment group, the negative control, and the positive control, respectively.

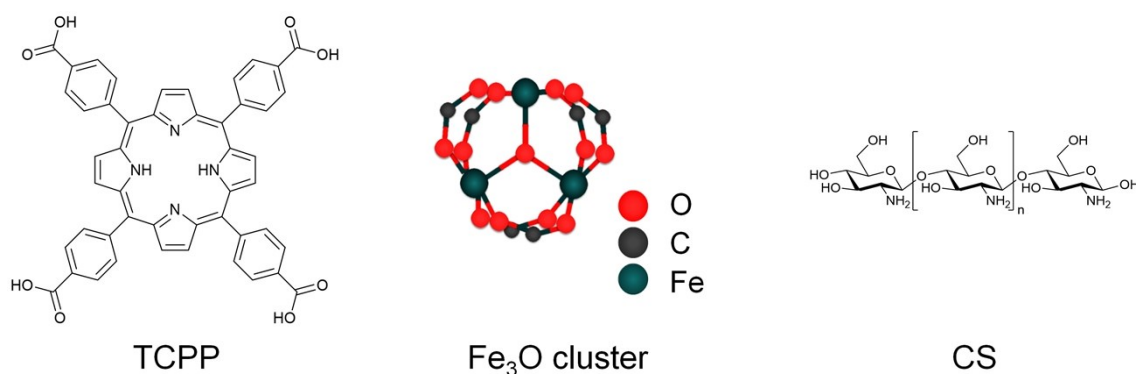


Figure S1. Schematic illustration of the structures of TCPP, Fe_3O cluster and CS.

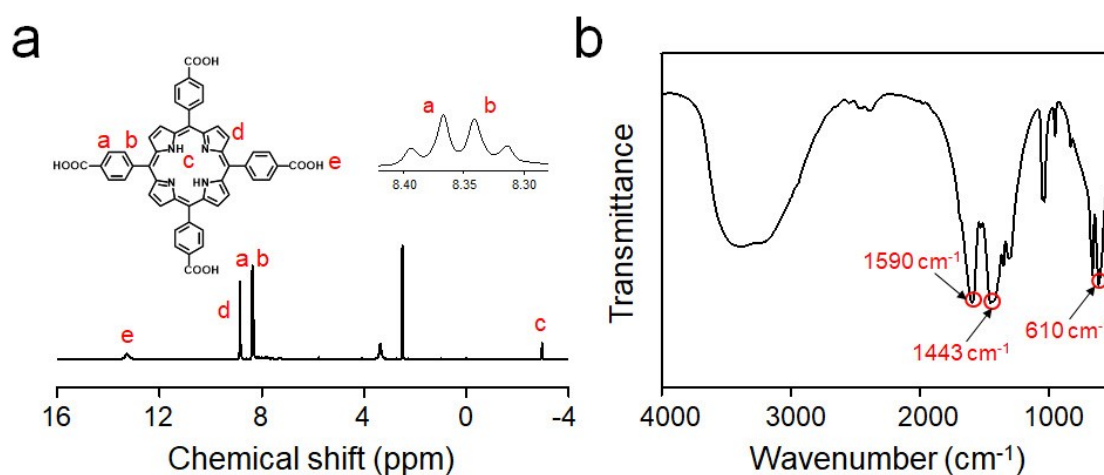


Figure S2. (a) ^1H NMR spectrum (300 MHz, DMSO, room temperature) of TCPP. (b) FT-IR spectra of Fe_3O cluster.

^1H -NMR spectrum of TCPP as shown was consistent with the literature reports.¹ ^1H NMR (300 MHz, DMSO): δ 13.21 (s, 4H, Ar-COOH), 8.85 (s, 8H, Pyr-H), 8.38 (d, $J = 8.0$ Hz, 8H, Ar-H), 8.32 (d, $J = 8.1$ Hz, 8H, Ar-H), -2.92 (bs, 2H, Pyr-NH). By recording the FT-IR spectrum of $[\text{Fe}_3\text{O}(\text{OOCCH}_3)_6\text{OH}] \cdot 2\text{H}_2\text{O}$, we found that the absorption peak of 1590 cm^{-1} and 1443 cm^{-1} which corresponded to the carboxylate radical, and the absorption peak of the Fe_3O was in 610 cm^{-1} .⁴

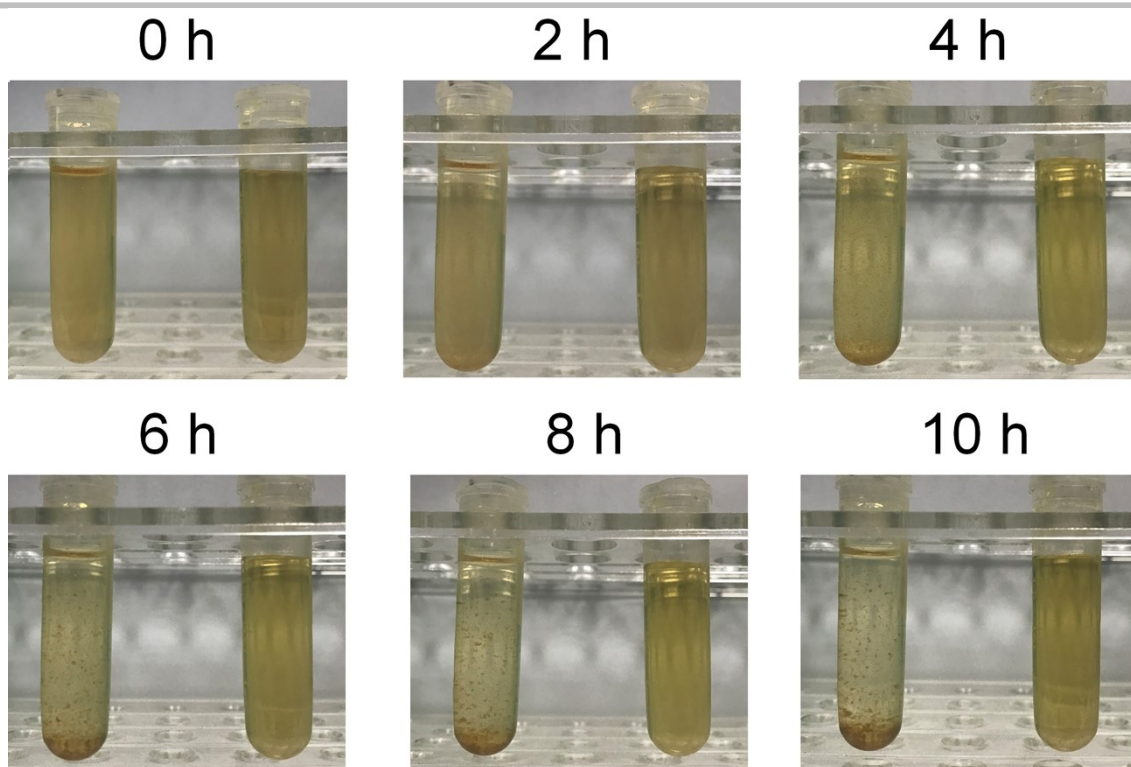


Figure S3. Dispersibility testing of Fe-TCPP NPs (left) and Fe-TCPP@CS NPs (right) at pH=5.5.

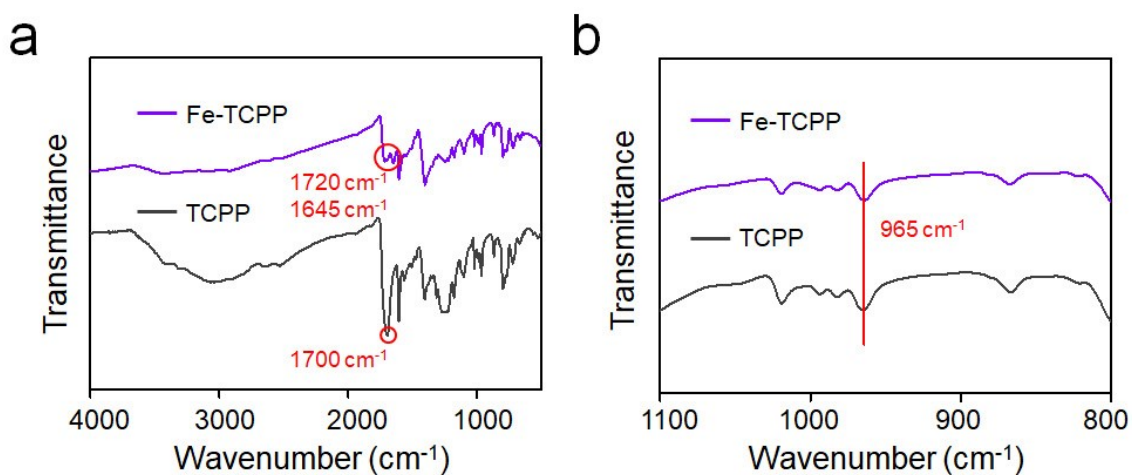


Figure S4. (a) FT-IR spectra of TCPP and Fe-TCPP. (b) is the enlarged part of (a)

By recording the Fourier transform infrared (FTIR) spectrum of Fe-TCPP, we found that the broad absorption in the range of 2500-3300 cm^{-1} , which corresponded to the hydroxyl group of COOH of free TCPP, disappeared, whereas the absorption peak of the carbonyl group went from 1700 cm^{-1} to two new peaks at 1720 and 1645 cm^{-1} (Figure S4a). These results indicated the formation of ionic bonds between COO^- and Fe^{3+} , consistent with data in previous reports.^{5,6} The N-H stretching vibration of TCPP at 965 cm^{-1} was still remained (Figure S4b), suggesting that iron ions were not coordinated in the porphyrin center of TCPP except as metal nodes.

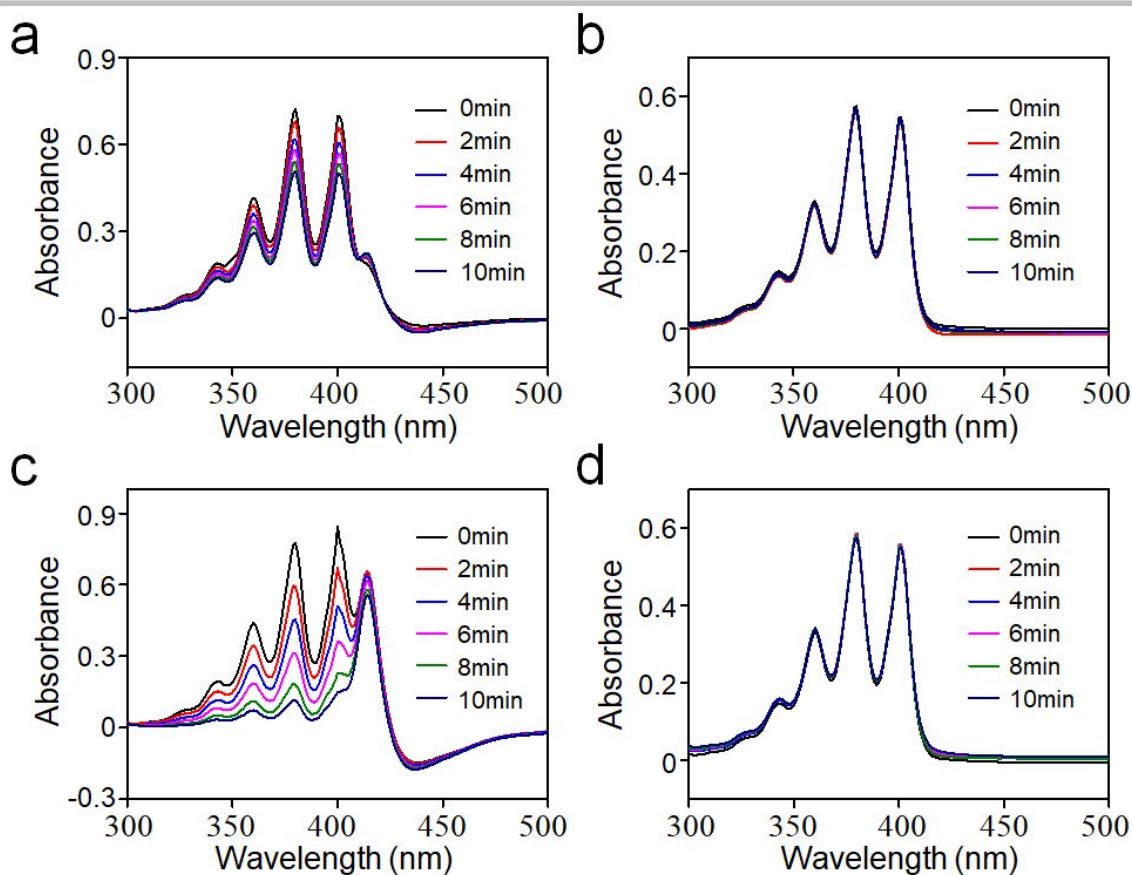


Figure S5. ABDA absorption spectra as a function of irradiation time after treating with (a) Fe-TCPP@CS + White light, (b) PBS + White light, (c) Fe-TCPP@CS + Laser and (d) PBS + Laser.

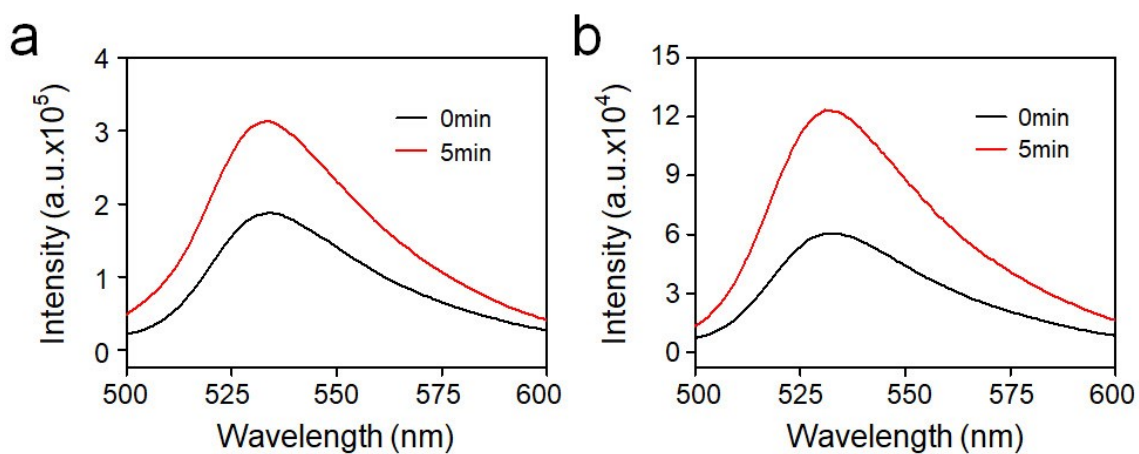


Figure S6. Fluorescence spectra of only SOSG upon white light irradiation (a) and laser irradiation (b) for 0 and 5 min.

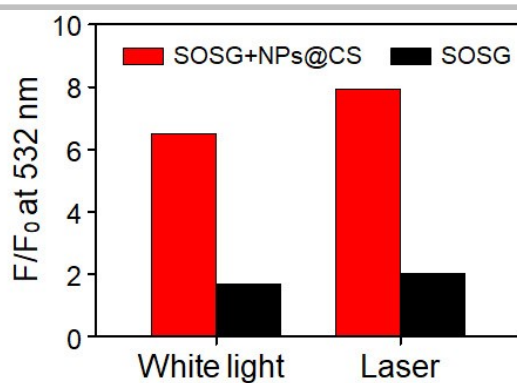


Figure S7. Relative fluorescence spectra of SOSG at 532 nm.

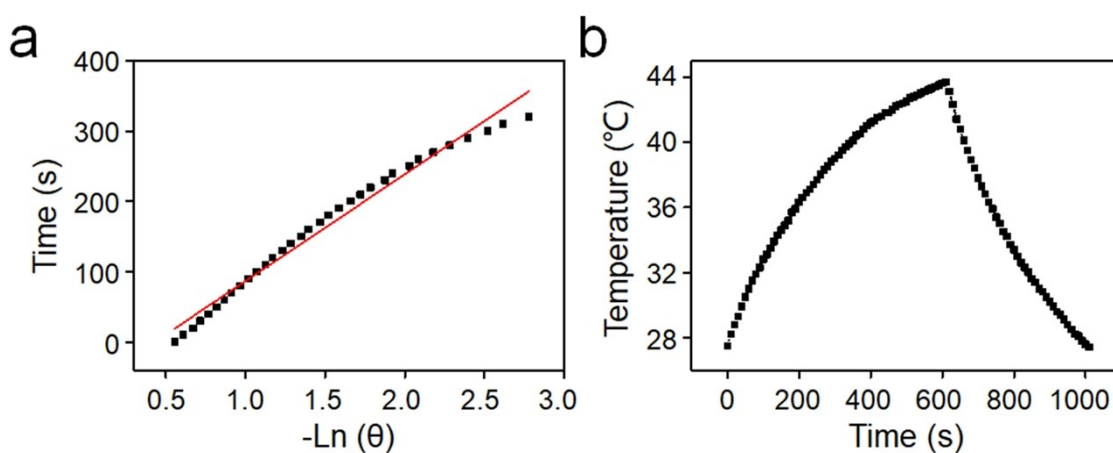


Figure S8. Calculation of the photothermal-conversion efficiency for Fe-TCPP@CS. (a) τ_s determination by the slope of the linear time data versus $-\ln(\theta)$ obtained from the cooling period of Figure S8b. (b) Temperature changes of an aqueous solution of Fe-TCPP@CS under irradiation of 635 nm laser for certain periods, and then the laser was turned off.

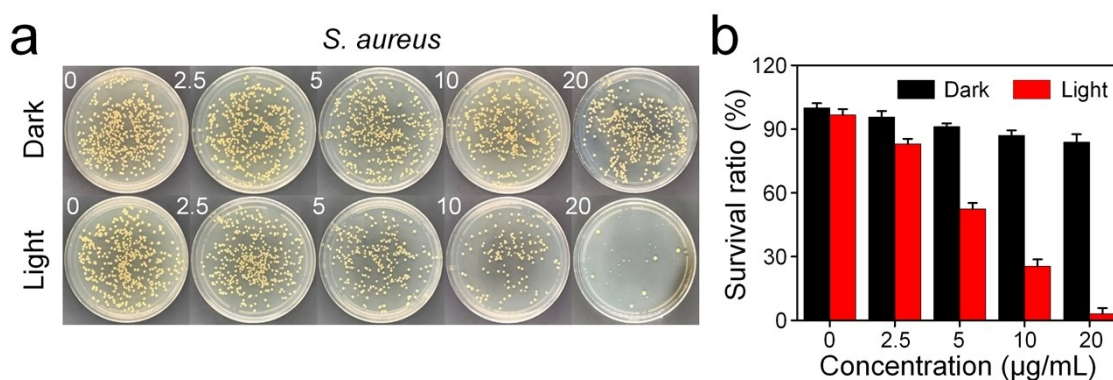


Figure S9. Dependence of bacterial survival rate on the concentration of Fe-TCPP@CS NPs under white light irradiation. Photographs of the bacterial colonies formed by (a) *S. aureus* treated with different concentrations of Fe-TCPP@CS. (b) is the survival rates corresponding to (a), respectively.

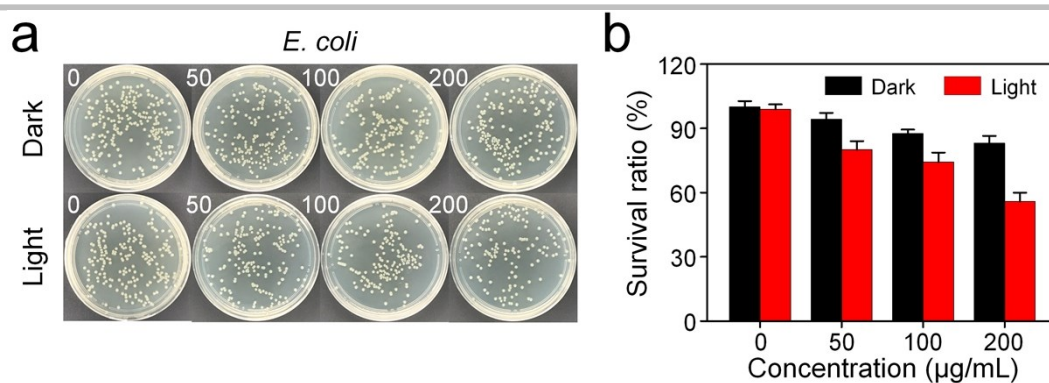


Figure S10. Dependence of bacterial survival rate on the concentration of Fe-TCPP@CS NPs under white light irradiation. Photographs of the bacterial colonies formed by (a) *E. coli* treated with different concentrations of Fe-TCPP@CS NPs. (b) is the survival rates corresponding to (a), respectively.

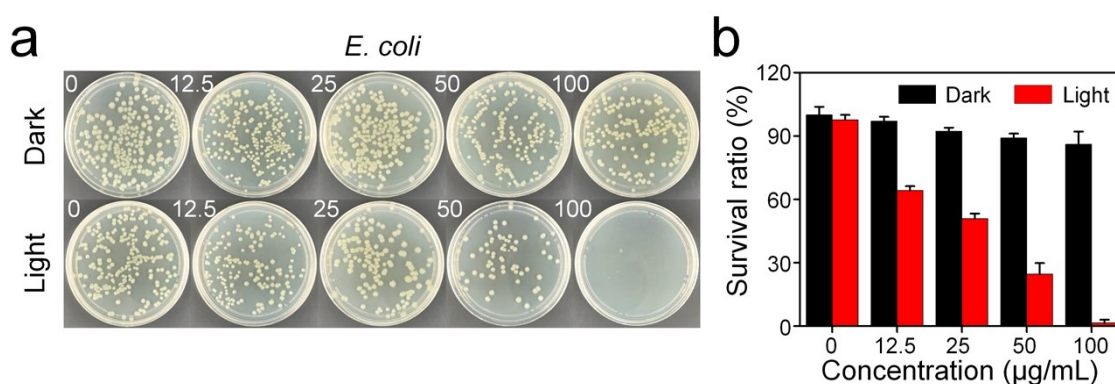


Figure S11. Dependence of bacterial survival rate on the concentration of Fe-TCPP@CS NPs under laser irradiation. Photographs of the bacterial colonies formed by (a) *E. coli* treated with different concentrations of Fe-TCPP@CS NPs. (b) is the survival rates corresponding to (a), respectively.

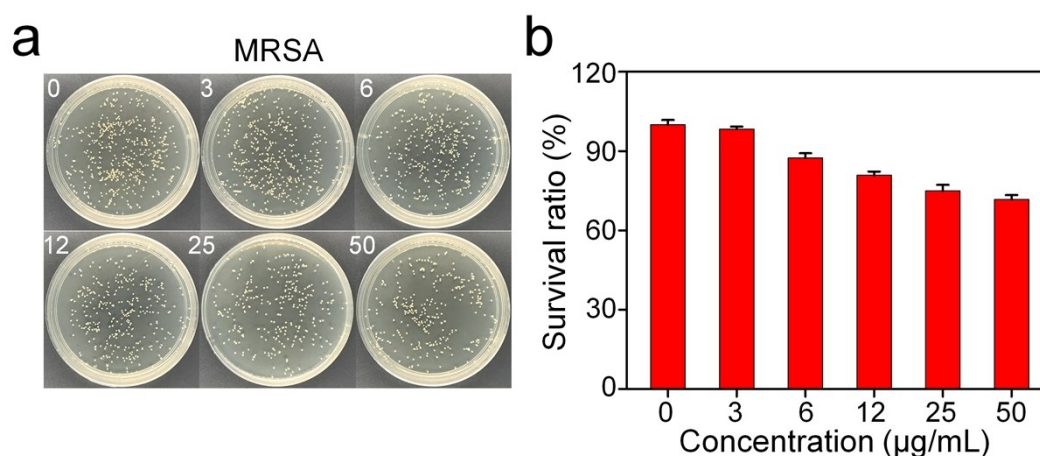


Figure S12. Dependence of MRSA survival rate on the concentration of Fe-TCPP@CS NPs in the dark. Photographs of the bacterial colonies formed by (a) MRSA in different concentrations of Fe-TCPP@CS NPs. (b) the survival rates of MRSA corresponding to (a), respectively.

The colonies of the bacteria were slightly decreased with the concentrations of Fe-TCPP@CS NPs increasing in the dark, which was attributed to the antimicrobial effect of CS against MRSA.

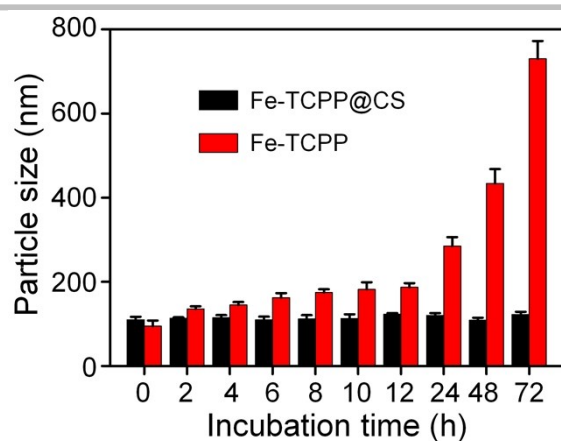


Figure S13. The DLS of Fe-TCPP@CS and Fe-TCPP NPs incubated at pH=5.5.

The stability of the Fe-TCPP@CS NPs after modification was improved at pH = 5.5, as increased production of acids (e.g. lactic acid) causes bacterial growth medium to be acidic, because CS could be fully dissolved in weak acid and improve the stability of NPs.

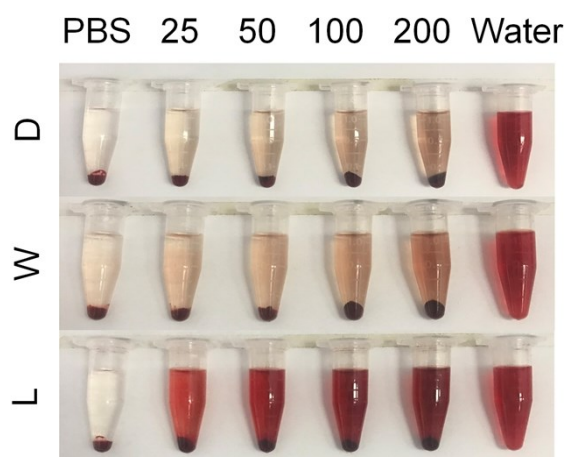


Figure S14. Relative Hemolysis photographs of PBS, water and different concentrations of Fe-TCPP@CS NPs. (D, W and L are shorthand for Dark, White light, and Laser respectively.)

References

- 1 K. Lu, C. He, N. Guo, C. Chan, K. Ni, R. R. Weichselbaum and W. Lin, *J Am Chem Soc*, 2016, **138**, 12502-12510.
- 2 X. Fang, L. Jiao, R. Zhang and H. L. Jiang, *ACS Appl Mater Interfaces*, 2017, **9**, 23852-23858.
- 3 D. K. Roper, W. Ahn and M. Hoepfner, *Journal of Physical Chemistry C*, 2007, **111**, 3636-3641.
- 4 M. K. Johnson, D. B. Powell and R. D. Cannon, *Spectrochimic. Acta*, 1981, **11**, 995-1006.
- 5 Z. Dong, L. Feng, Y. Hao, Q. Li, M. Chen, Z. Yang, H. Zhao and Z. Liu, *Chem*, 2020, DOI: 10.1016/j.chempr.2020.02.020.
- 6 R. Rahimi, S. Shariatinia, S. Zargari, M. Yaghoubi Berijani, A. Ghaffarinejad and Z. S. Shojaie, *RSC Advances*, 2015, **5**, 46624-46631.